Available online at www.sciencedirect.com
ScienceDirect
International Journal of Heat and Mass Transfer 50 (2007) 3684–3689
International Journal of HEAT and MASS TRANSFER
www.elsevier.com/locate/ijhmt

Technical Note

Numerical investigation of natural convection in an inclined enclosure filled with porous medium under magnetic field

Q.W. Wang *, M. Zeng, Z.P. Huang, G. Wang, H. Ozoe

State Key Laboratory of Multiphase Flow in Power Engineering, Xi'an Jiaotong University, Xi'an 710049, China

Received 13 September 2006; received in revised form 23 January 2007
Available online 5 April 2007

Abstract

In the present study, natural convection of fluid in an inclined enclosure filled with porous medium is numerically investigated in a strong magnetic field. The physical model is heated from left-hand side vertical wall and cooled from opposing wall. Above this enclosure an electric coil is set to generate a magnetic field. The Brinkman–Forchheimer extended Darcy model is used to solve the momentum equations, and the energy equations for fluid and solid are solved with the local thermal non-equilibrium (LTNE) models. Computations are performed for a range of the Darcy number from 10^{-5} to 10^{-1}, the inclination angle from 0 to $\pi/2$, and magnetic force parameter γ from 0 to 100. The results show that both the magnetic force and the inclination angle have significant effect on the flow field and heat transfer in porous medium.

Keywords: Natural convection; Porous medium; Magnetic force; Local thermal non-equilibrium (LTNE)

1. Introduction

The research of natural convection in porous medium has been conducted widely in recent years, which involves post-accidental heat removal in nuclear reactors, cooling of radioactive waste containers, the migration of moisture through the air contained in fibrous insulations, the dispersion of chemical pollutants through water-saturated materials, heat exchangers, solar power collectors, grain storage, food processing, energy efficient drying process, to name of a few. Nield and Bejan [1] and Ingham and Pop [2] contributed to a wide overview of this important area in heat transfer of porous medium. There are many open literature related to natural convection in rectangular porous enclosures [3–7]. The study of thermal convection in inclined enclosures is motivated by a desire to find out any effects of the slope on thermally driven flows which are found in many engineering applications. Caltagirone and Bories [8] studied the stability criteria of free convective flow in an inclined porous layer. Vasseur et al. [9] investigated the natural convection in a thin inclined porous layer exposed to a constant heat flux and in other contributions by Sen et al. [10] and Baytas [11]. The aforementioned natural convection is only related to buoyancy-driven flows. As is known recently, the magnetic force is another driving force, which is proportional to the magnetic susceptibility of the fluid and approximately proportional to the gradient of the square of magnetic induction. Natural convection under magnetic force has been examined quite recently by some investigators [12–15]. However, almost no attentions are paid on the combined effects of both magnetic and gravitational forces on the natural convection in porous medium. Furthermore, magnetic force has received more attention in the field of metallic materials, and less in the field of non-metallic materials. It is acceptable only when the magnetic force is small. With the increase of magnetic field intensity, the magnetic force has more effects on the non-metallic materials. The application of strong magnetic field for porous medium may be found in the field of medical

* Corresponding author. Tel./fax: +86 29 8266 3502.
E-mail address: wangqw@mail.xjtu.edu.cn (Q.W. Wang).

0017-9310/$ - see front matter © 2007 Elsevier Ltd. All rights reserved.
doi:10.1016/j.ijheatmasstransfer.2007.01.045

Nomenclature

a_{sf}	specific surface area of the porous medium (m^{-1})
$\underline{b}_0$	uniform magnetic induction (T)
$\underline{b}$	magnetic induction (T)
B	dimensionless magnetic flux
c_p	specific heat at constant pressure ($J\,kg^{-1}\,K^{-1}$)
d_p	sphere particle diameter (m)
Da	Darcy number (K/H^2)
F	geometric function
g	gravitational acceleration ($m\,s^{-2}$)
h	distance between coil and the center of the enclosure (m)
h_{sf}	solid-to-fluid heat transfer coefficient ($W\,m^{-2}\,K^{-1}$)
H	side length of the enclosure (m)
i	electric current in a coil (A)
k	thermal conductivity ($W\,m^{-1}\,K^{-1}$)
K	permeability (m^2)
Nu	Nusselt number, Eq. (6)
p	pressure (Pa)
P	dimensionless pressure
Pr	Prandtl number, $Pr = \nu_f/\alpha_m$
r	distance from coil segment to a point (m)
R	coil radius (m) in Fig. 1, dimensionless distance in Eq. (3)
Ra	Rayleigh number, $Ra = gH^3\beta(T_h - T_c)/(\nu\alpha_m)$
$\vec{s}$	tangential vector of a coil
T	temperature (K)
u, v, w	velocity components ($m\,s^{-1}$)
U, V, W	dimensionless velocity components
x, y, z	x-, y-, z-coordinates
X, Y, Z	dimensionless coordinates

Greek symbols

α	inclination angle, radian
α_m	thermal diffusivity ($m^2\,s^{-1}$)
β	thermal expansion coefficient (K^{-1})
γ	dimensionless magnetic strength parameter
δ	mass fraction of oxygen
θ	dimensionless temperature
μ	viscosity of gas ($kg\,m^{-1}\,s^{-1}$)
μ_m	magnetic permeability ($m\,kg\,(s\,A)^{-2}$)
ν	kinematic viscosity ($m^2\,s^{-1}$)
ρ	density ($kg\,m^{-3}$)
χ	mass magnetic susceptibility of fluid ($m^3\,kg^{-1}$)
Λ	dimensionless thermal conductivity
ϕ	porosity
ξ	dimensionless solid-to-fluid heat transfer coefficient

Subscripts

f	fluid
ef	effective properties for fluid
s	solid
es	effective properties for solid

treatment such as magnetic resonance imaging and/or attachment of small magnets on the tissue surface to reduce the muscle ache. The details of these effects on the metabolism have not been clarified yet. However, there may be plenty of applications in the near future in the field of engineering operations. Thus, as a first trial we intend to study the effects of magnetic force on the natural convection in porous enclosure. The heat and flow characteristics are studied on the effect of the inclination angle (α), Darcy number (Da), and magnetic force parameter (γ). The porous medium is supposed to consist of air (paramagnetic fluid $\gamma > 0$) and soda lime, and the corresponding thermal and magnetic properties can be found in Refs. [7,13].

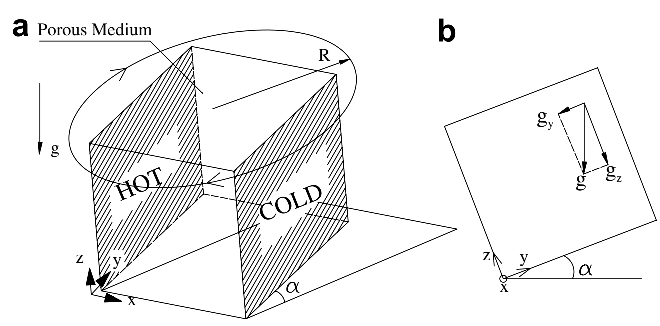

Fig. 1. Schematic diagram of the physical system.

2. System considered

The schematic view of the problem is shown in Fig. 1. The cubic enclosure is filled with saturated porous medium. One of a vertical wall is isothermally heated and an opposite wall is cooled and the other walls are thermally insulated. A coil is set above and coaxially with the enclosure to produce magnetic field. The hot and cold walls are kept vertically while the magnetic force field is inclined at an angle of α from a gravitational direction. Fig. 1b shows schematics of the gravity force separated in the Y- and Z-coordinate with the X-axis kept horizontal and the magnetic force is mostly in the Z-coordinate. The inclination angle (α) varies from 0 to $\pi/2$. In the present study, the size of the cubic enclosure H is 0.064 m, the radius R of coil is 0.05 m and the distance h between coil and the center of the cubic is 0.032 m (see Fig. 1). However, the qualitative results are not limited for these combinations of parameters.

3. Model equations and validation

In the model development, the following assumptions are adopted: the fluid is an incompressible Newtonian fluid, no phase change occurs and the process is in a steady state; the Boussinesq approximation is adopted; the porous medium is isotropic; the Joule heating; the effect of magnetic field on heating is negligible; porosity ϕ is assumed uniform throughout the enclosure and thermal dispersion is omitted.

The dimensionless governing equations in Cartesian coordinates for the present study then take the following form.

Continuity equation:

$$\nabla \cdot \vec{V} = 0. \tag{1}$$

Momentum equation:

$$\frac{1}{\phi^2}\vec{V}\cdot\nabla\vec{V} = -\nabla P + \frac{Pr}{\phi}\nabla^2\vec{V} - \frac{Pr}{Da}\vec{V} - \frac{F}{\sqrt{Da}}|\vec{V}|\vec{V} + RaPr\theta_{\mathrm{f}}\left\{-\gamma\nabla B^2 + \begin{bmatrix} 0 \\ \sin\alpha \\ \cos\alpha \end{bmatrix}\right\}. \tag{2}$$

The geometric function F can be represented as in Ref. [3], and the introduction of magnetic term can be found in Refs. [12,17], and the magnetic induction B can be defined by *Biot–Savart's law* [12]:

$$\vec{B} = -\frac{1}{4\pi}\int \frac{\vec{R}\times \mathrm{d}\vec{s}}{R^3}. \tag{3}$$

Fluid phase energy equation [3]:

$$(1 + \Lambda^{-1})\vec{V}\cdot\nabla\theta_{\mathrm{f}} = \nabla^2\theta_{\mathrm{f}} + \xi(\theta_{\mathrm{s}} - \theta_{\mathrm{f}}). \tag{4}$$

Solid phase energy equation [3]:

$$0 = \nabla^2\theta_{\mathrm{s}} + \Lambda\xi(\theta_{\mathrm{f}} - \theta_{\mathrm{s}}). \tag{5}$$

The following dimensionless variables and reference values are employed in the above dimensionless equations:

$$X = \frac{x}{H},\quad Y = \frac{y}{H},\quad Z = \frac{z}{H},\quad U = \frac{uH}{\alpha_{\mathrm{m}}},$$

$$V = \frac{vH}{\alpha_{\mathrm{m}}},\quad W = \frac{wH}{\alpha_{\mathrm{m}}},\quad P = \frac{pH^2}{\rho_{\mathrm{f}}\alpha_{\mathrm{m}}^2},$$

$$\theta = \frac{T - T_0}{T_{\mathrm{h}} - T_{\mathrm{c}}},\quad T_0 = \frac{T_{\mathrm{h}} + T_{\mathrm{c}}}{2},\quad Pr = \frac{\nu_{\mathrm{f}}}{\alpha_{\mathrm{m}}},$$

$$Ra = \frac{gH^3\beta(T_{\mathrm{h}} - T_{\mathrm{c}})}{\nu\alpha_{\mathrm{m}}},\quad \alpha_{\mathrm{m}} = \frac{k_{\mathrm{ef}} + k_{\mathrm{sf}}}{(\rho c_{\mathrm{p}})_{\mathrm{f}}},$$

$$Da = \frac{K}{H^2},\quad \Lambda = \frac{k_{\mathrm{ef}}}{k_{\mathrm{es}}},\quad \xi = \frac{a_{\mathrm{sf}}h_{\mathrm{sf}}H^2}{k_{\mathrm{ef}}},$$

$$B = \frac{b}{b_0},\quad b_0 = \mu_{\mathrm{m}}i/H,\quad S = s/H,$$

$$R = r/H,\quad \gamma = \frac{\chi_0\delta b_0^2}{g\mu_{\mathrm{m}}H},$$

where $k_{\mathrm{ef}} = \phi k_{\mathrm{f}}$, $k_{\mathrm{es}} = (1-\phi)k_{\mathrm{s}}$. The permeability of the porous medium K, the specific surface area a_{sf} and the fluid-to-solid heat transfer coefficient h_{sf} are determined as in Ref. [16].

The boundary conditions for three velocity components are set to zero at all solid walls. The temperature boundary conditions are as follows:

$$\begin{aligned}
&\theta_{\mathrm{f}} = \theta_{\mathrm{s}} = 0.5 && \text{at } X = 0;\\
&\theta_{\mathrm{f}} = \theta_{\mathrm{s}} = -0.5 && \text{at } X = 1;\\
&\tfrac{\partial\theta_{\mathrm{f}}}{\partial Y} = \tfrac{\partial\theta_{\mathrm{s}}}{\partial Y} = 0 && \text{at } Y = 0 \text{ and } 1;\\
&\tfrac{\partial\theta_{\mathrm{f}}}{\partial Z} = \tfrac{\partial\theta_{\mathrm{s}}}{\partial Z} = 0 && \text{at } Z = 0 \text{ and } 1.
\end{aligned}$$

The overall heat transfer characteristics are described by the average Nusselt number of the hot wall, which is defined as follows [7] :

$$Nu_{\mathrm{m}} = -\int_0^1\int_0^1 \phi\left(-\frac{\partial\theta_{\mathrm{f}}}{\partial X} - \Lambda^{-1}\frac{\partial\theta_{\mathrm{s}}}{\partial X}\right)_{X=0}\mathrm{d}Y\,\mathrm{d}Z. \tag{6}$$

A 3D, uniform and staggered grid is used with a control-volume formulation for the discretization. Pressure correction and velocity correction are implemented in accordance with the SIMPLE algorithm [16] to achieve a converged solution. The discretized algebraic equations are solved by the tri-diagonal matrix algorithm (TDMA). Relaxation factors of about 0.2–0.5 are used for the velocity components, while relaxation factors of about 0.5–0.7 are adopted for the temperature and pressure corrections. In all the computations, the porosity ϕ is set as 0.9. For convergence criteria, the relative variations of the temperature and velocity between two successive iterations are demanded to be smaller than the previously specified accuracy levels of 5.0×10^{-5}.

Before proceeding further, it is necessary to ascertain the reliability and accuracy of the present numerical model and the code developed. Five sets of grids, $10 \times 10 \times 10$, $20 \times 20 \times 20$, $30 \times 30 \times 30$, $40 \times 40 \times 40$, and $50 \times 50 \times 50$, are employed for $Ra = 10^4$, $\gamma = 100$, $\alpha = \pi/4$ and $Da = 10^{-1}$; the case with $40 \times 40 \times 40$ grids is used for taking both the accuracy and convergence rate into account. Also, quantitative comparisons are made respectively with the results to the test problems as computed in [1,15], and the average deviation of Nusselt numbers is 1.89% and 1.38%, respectively. The two test problems combined together illuminate that present simulation method is correct on flow and heat transfer for natural convection in enclosure with porous medium under both gravitational and magnetic forces.

4. Results and discussion

4.1. Nature of flow and temperature field

The results show that the flow and temperature field are very complex. Fig. 2 shows the effect of γ number on the magnetic force vectors, velocity vectors, fluid and solid temperature contours in the vertical cross-section at

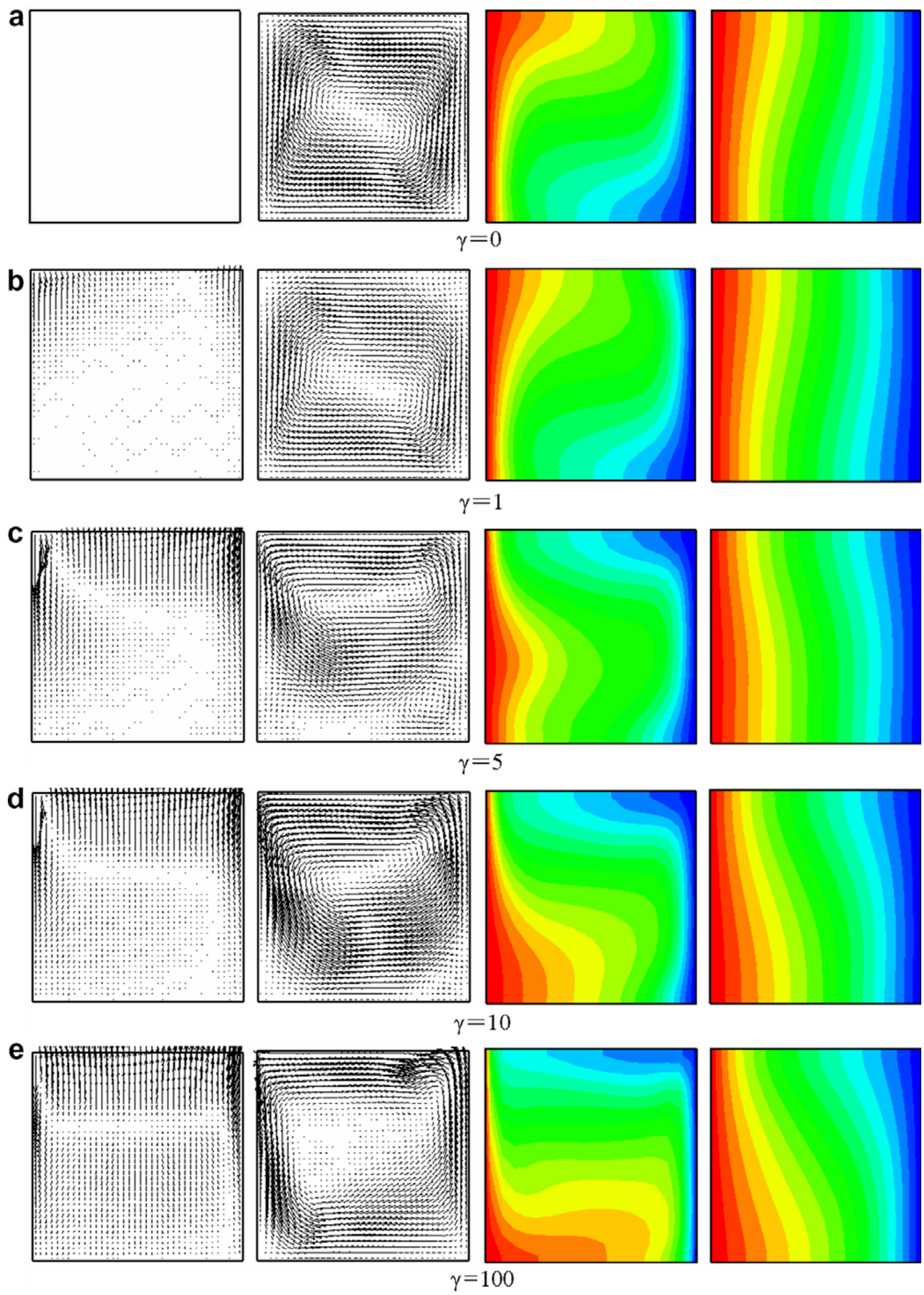

Fig. 2. Computed profiles in a plane $Y = 0.5$ at $Da = 10^{-1}$, $\alpha = \pi/4$, $Ra = 10^4$.

$Y = 0.5$, $Da = 10^{-1}$, $\alpha = \pi/4$ and $Ra = 10^4$. The left-hand side wall is hot and the right-hand side wall is cold in each graph. Without a magnetic field ($\gamma = 0$), the hot air rises up along the left-hand side hot wall and descends along the right-hand side cold wall as seen in fluid isothermal contours at $\gamma = 0$. The model equation includes the effect of magnetic force in which the magnetic susceptibility of paramagnetic fluid is inversely proportional to its temperature according to the Curie's law [17]. When there is a magnetic field, the magnetic force repels the left-hand side hot air (relatively at higher temperature and smaller magnetic susceptibility than that at the average temperature air and is repelled comparatively). On the other hand, the cold air near the right-hand side wall is at lower temperature, and has larger magnetic susceptibility and is easily to be attracted to the strong magnetic field than that at the average temperature. Because of this characteristic, the air is repelled downward near the left-side and attracted upward near the right-side. At $\gamma = 0$ and 1, the hotter fluid along the left-hand side wall ascends upward, the colder fluid along the right-hand side wall descends downward due to the usual gravitational buoyancy force, which forms a clockwise flow. At $\gamma = 5$, the magnetic force becomes large and the hot fluid along the left-hand side hot wall is repelled downward at the upper half height and proceeds toward the cold wall where fluid is attracted upward along the cold plate, which forms an anticlockwise flow in the upper half region. In the lower half enclosure, usual gravitational convection occurs ascending along the hot left-hand side wall and descending along the right-hand side wall. At $\gamma = 10$ and 100, the magnetic force becomes very large and the flow is just reversed to the usual gravitational convection at $\gamma = 0$. The convection is totally downward along the hot wall and upward along the cold wall. This also suggests that the usual natural convection can be completely reversed with employing the magnetic force field. For the temperature field, with the increase of magnetic force, even at $\gamma = 0$, the temperature difference between the solid and liquid is greatly increased, so the LTNE models is important in simulating the heat transfer in porous medium when there is a strong magnetic field.

4.2. Effects of Darcy number

Computations are carried out for fluids with Darcy number varying from 10^{-5} to 10^{-1} at $Ra = 10^4$. The values of the average Nusselt number are shown in Fig. 3. It is found that, with other parameters unchanged, Darcy number has a certain effect on the heat transfer and fluid flow. When the Darcy number is small, the magnitude of magnetic force has little effect on the heat transfer rate. The results clearly suggest that the reduction in the value of Da causes the flow to eventually cease in the bulk of the enclosure. The presence of a porous medium subsequently

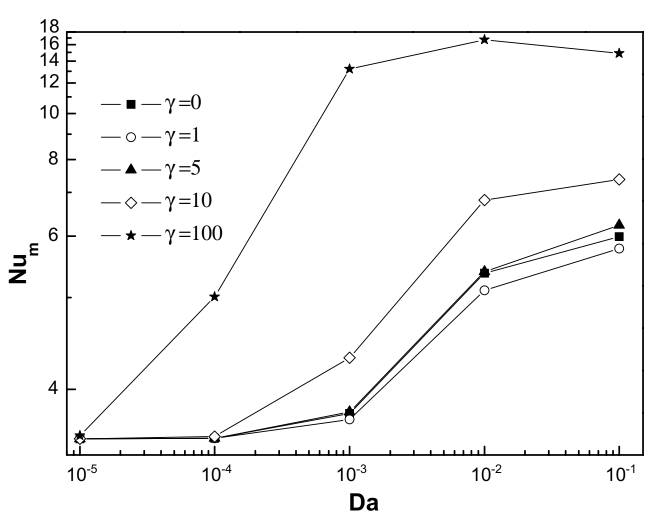

Fig. 3. Average Nusselt numbers at $Ra = 10^4$, $\alpha = \pi/4$.

Table 1
Average Nusselt numbers at various values of γ number and inclination angle α ($Da = 10^{-1}$, $Ra = 10^4$)

γ	α				
	0	$\pi/6$	$\pi/4$	$\pi/3$	$\pi/2$
0	5.801	5.813	5.815	5.813	5.800
1	5.425	5.507	5.596	5.689	5.866
5	5.196	5.700	6.036	6.311	6.743
10	6.381	6.683	7.142	7.391	7.798
100	14.366	14.403	14.447	14.501	14.623

brings about suppression in the thermal currents of the flow, which causes a reduction in the overall heat transfer between the hot and cold walls. With the increase of Darcy number, the overall heat transfer is enhanced gradually. When γ equals to 1, the average Nusselt number is less than that when $\gamma = 0$ since the magnetic force is against to the gravitational force. However, with further increase in the γ number, the magnetic force overcomes the gravitational force and the average Nusselt number exceeds that of usual natural convection ($\gamma = 0$). When the coil is placed above the enclosure, the magnetic force acts against the gravity force and the usual natural convection is gradually restrained with the increase of γ number, which can be observed in Fig. 2.

4.3. Effects of inclination angle

In order to examine the effects of inclination angle, computations are carried out for a fluid with the inclined angle (α) varying from 0 to $\pi/2$, while other geometric parameters remained unchanged. Numerical results are obtained for $Da = 10^{-1}$ and $Ra = 10^4$ at $\gamma = 0$–100. Table 1 illustrates the effects of inclination angle on the average Nusselt number. At $\gamma = 0$, it can be seen that the Nusselt number attains the maximum value at $\alpha = \pi/4$, because the effective height of the hot and cold walls take the maximum value at this orientation. However, there is little difference among the magnitude of the average Nusselt number at different inclination angle. When there exists magnetic field ($\gamma > 0$) in the enclosure, the heat transfer is enhanced with the increase of the inclination angle. The average Nusselt number takes minimum value at about $\gamma = 5$ for $\alpha = 0$, at $\gamma = 1$ for $\alpha = \pi/6$–$\pi/3$ and at $\gamma = 0$ for $\alpha = \pi/2$. This is because the magnetic force is against to the gravitational buoyancy force at α less than $\pi/2$, but at $\alpha = \pi/2$ they are no more against each other and the average Nusselt number increases with γ.

5. Conclusions

The effect of magnetic force for the natural convection of fluid in an inclined cubic enclosure filled with porous medium is studied in detail. The study makes use of generalized form of the momentum equation in describing the flow field. Furthermore, the local thermal non-equilibrium models (LTNE) are utilized to describe the thermal response of the porous enclosure. The work covers a wide range of parameters. Complicated flow and temperature fields and the effects of some parameters are revealed. The major findings are as follows:

(1) When Darcy numbers are small, conduction becomes dominated.
(2) With the increase of magnetic strength, the average Nusselt number has a transition point. Here, the magnetic force acts against the gravitational force and net accelerating force becomes smaller that without magnetic field, and the average Nusselt numbers decrease herewith. However, with the increase of γ number, the magnetic force overcomes the gravitational force and makes the fluid flow reversely, and the average Nusselt numbers increase again. The temperature difference between solid phase and fluid phase is quite different and thus it is necessary to use the local thermal non-equilibrium models for such kind of problem.
(3) At $\gamma = 0$, the average Nusselt number attains the maximum value at inclination angle $\alpha = \pi/4$. When $\gamma > 0$, the heat transfer of the inclined porous enclosure is enhanced with the increase of inclination angle (α).

Acknowledgement

We would like to acknowledge financial support for this work provided by the National Natural Science Foundation of China (No. 50521604).

References

[1] D.A. Nield, A. Bejan, Convection in Porous Media, second ed., Springer-Verlag, Inc., New York, 1999.
[2] D.B. Ingham, I. Pop, Transport Phenomena in Porous Media, Pergamon, Oxford, 1998.
[3] K. Vafai, Handbook of Porous Media, vol. II, Marcel Dekker, New York, 2004.
[4] V. Prasad, F.A. Kulacki, Convective heat transfer in a rectangular porous cavity effect of aspect ratio on flow structure and heat transfer, J. Heat Transfer 106 (1) (1984) 158–165.
[5] A.C. Baytas, I. Pop, Free convection in oblique enclosures filled with a porous medium, Int. J. Heat Mass Transfer 42 (6) (1999) 1047–1057.
[6] A.M. Al-Amiri, Natural convection in porous enclosures the application of the two-energy equation model, Numer. Heat Transfer A 41 (8) (2002) 817–834.
[7] T. Basak, S. Roy, T. Paul, I. Pop, Natural convection in a square cavity filled with a porous medium: Effects of various thermal boundary conditions, Int. J. Heat Mass Transfer 49 (7–8) (2006) 1430–1441.
[8] J.P. Caltagirone, S. Bories, Solutions and stability criteria of natural convective flow in an inclined porous layer, J. Fluid Mech. 155 (6) (1985) 267–287.
[9] P. Vasseur, M.G. Satish, L. Robillard, Natural convection in a thin inclined porous layer exposed to a constant heat flux, Int. J. Heat Mass Transfer 30 (3) (1987) 537–549.
[10] M. Sen, P. Vasseur, L. Robillard, Multiple steady states for unicellular natural convection in an inclined porous layer, Int. J. Heat Mass Transfer 30 (10) (1987) 2097–2113.
[11] A.C. Baytas, Entropy generation for natural convection in an inclined porous cavity, Int. J. Heat Mass Transfer 43 (12) (2000) 2089–2099.
[12] Hiroyuki Ozoe, Magnetic Convection, Imperial College Press, 2005.
[13] Ryoji Shigemitsu, Toshio Tagawa, Hiroyuki Ozoe, Numerical computation for natural convection of air in a cubic enclosure under combination of magnetizing and gravitational forces, Numer. Heat Transfer A 43 (5) (2003) 449–463.
[14] H.M. Park, W.S. Jung, Numerical solution of optimal magnetic suppression of natural convection in magneto-hydrodynamic flows by empirical reduction of modes, Comput. Fluids 31 (3) (2002) 309–334.
[15] Riki Noda, Masayuki Kaneda, Toshio Tagawa, Hiroyuki Ozoe, Magnetizing convection of air in a cubical enclosure with one magnetic coil either over the top wall or over the bottom wall, in Heat Transfer 2002: Proceedings of the Twelfth International Heat Transfer Conference, vol. 2, Grenoble, France, 2002, pp. 549–554.
[16] S.V. Patankar, Numerical Heat Transfer and Fluid Flow, Hemisphere/McGraw-Hill, New York, 1980.
[17] B. Bai, A. Yabe, J. Qi, N.I. Wakayama, Quantitative analysis of air convection caused by magnetic-fluid coupling, AIAA J. 37 (12) (1999) 1538–1543.